Predicting the COVID-19 Patients' Status Using Chest CT Scan Findings: A Risk Assessment Model Based on Decision Tree

Atefeh Talebi
Iran University of Medical Sciences
Nasrin Borumandnia
Shaheed Beheshti University of Medical Sciences
Ramezan Jafari
Baqiyatallah University of Medical Sciences
Mohamad Amin Pourhoseingholi
Shaheed Beheshti University of Medical Sciences https://orcid.org/0000-0002-0121-8031
Nematollah Jonaidi Jafari
Baqiyatallah University of Medical Sciences
Sara Ashtari
Shaheed Beheshti University of Medical Sciences Research Institute for Gastroenterology and Liver Diseases
Saeid Roozpeykar
Baqiyatallah University of Medical Sciences
Farshid R. Bashar
Hamedan University of Medical Science
Amir Vahedian-Azimi (Amirvahedian63@gmail.com)
Baqiyatallah University of Medical Sciences https://orcid.org/0000-0002-1678-7608

Research article

Keywords: Chest CT scan without contrast, coronavirus disease, COVID-19, disease outcome, decision tree

Posted Date: August 12th, 2020

DOI: https://doi.org/10.21203/rs.3.rs-56387/v1

Abstract

Background: The role of chest computed tomographic (CT) to diagnosis coronavirus disease-2019 (COVID-19) is still an open field to be explored. The aim of this study is to use non-contrast chest computed tomography (CT) scan as a helpful tool in diagnosis quantification and follow-up of patients with COVID-19.

Method: This study was performed on patients with COVID-19 who underwent chest CT scan at Baqiyatallah Hospital, Tehran, Iran. The age, gender, types of lesions, other specific signs of high-resolution computed tomography (HRCT), presence of diffuse opacity, underlying diseases, number of involved lobe and total opacity score of 1078 patients were evaluated. Decision tree (DT) model was used to analyze and establish a risk assessment model of critical and non-critical situation.

Results: The bilateral distribution and multifocal lung involvement were 165 (97.6%) and 766 (84.3%) in critical patients, respectively. According to DT model, total opacity score, age, lesion types and gender were statistically significant predictors in critical patients. Moreover, the results showed that the accuracy, sensitivity and specificity of the DT model were 93.3%, 72.8% and 97.1%, respectively.

Conclusions: The presented algorithm demonstrates the factors affecting the patient's condition. Also the model can predict the critical or non-critical situation of new cases. In addition, this model has the potential characteristics for clinical applications and can also identify high-risk subpopulations that need specific prevention.

Background:

The novel coronavirus disease 2019 (COVID-19) known as viral pneumonia, which has been emerged at the Huanan Seafood Market, Wuhan, China (Kanne, 2020, Rodriguez-Morales et al., 2020). The WHO has introduced this virus as a pandemic disease. Nowadays, COVID-19 is affecting more than 210 countries around the world. As of May 11, 2020, a total of 4,196,193 confirmed COVID-19 cases, 1,500,181 recovered cases with 284,033 deaths have been reported in the world. While the statistics demonstrated that the trend of mortality have declined in China and is rising in the world as well as in Iran (Moftakhar and Seif, 2020). The first experience of the disease in Iran was identified in the Qom city on February 19, 2020 (Muniz-Rodriguez et al., 2020). Afterwards, the disease has been quickly affecting a growing number of people throughout the country until 3 May when the total number of confirmed patients has increase to 97,424 (2020).

The COVID-19 can lead to respiratory infection, liver disease, gastrointestinal and neurological disorders (Musa, 2020, Boettler et al., 2020). In addition, the virus can cause severe acute respiratory syndrome such as pneumonia, pulmonary edema, acute respiratory distress syndrome (ARDS) (Matthay et al., 2019). Therefore, the non-contrast chest computed tomography (CT) scan may be applied as a helpful tool in diagnosis quantification and follow-up of patients with COVID-19. The lungs of patients with COVID-19 symptoms had certain visual hallmarks, such as ground-glass opacities (GGO) and and areas

of increased lung density called consolidation (Kim, 2020). Furthermore, greater severity of disease with increasing time from onset of symptoms showed other findings as specific signs that includes, linear opacities, crazy-paving pattern, reverse halo sign, pleural effusion, intralesional traction bronchiectasis and lymphadenopathy (Bhat et al., 2020, Li, 2020).

The Classification and Regression Tree (CART) decision tree (DT) analysis is a data mining technique that used for establishing classification systems based on multiple covariates or for developing prediction algorithms for a target variable (Song and Lu, 2015). The algorithm has numerous merits such as it can split sequential data into the best predictive group (Zimmerman et al., 2016). The aim of the retrospective study, with such a large sample size population, was to apply the CART decision tree model to predict the status (critical/ non-critical status) of patients with COVID-19 based on chest CT findings. Also, the model is able to predict whether the conditions of new patient are critical or non-critical. Additionally, receiver operating characteristic (ROC) analysis was applied to assess the ability of DT model for prediction the critical and non-critical condition.

Methods:

Study design and patients

In the retrospective study, we collected both demographic characteristics and radiologic information of 1078 patients with COVID-19 who referred to Baqiyatallah Hospital, Tehran, Iran from March to April 2020. Positive results on a reverse-transcriptase–polymerase-chain-reaction (RT-PCR) assay of a specimen obtained on a nasopharyngeal swab indicated was the confirmation of COVID-19. According to patients' clinical outcomes, the individuals were divided into two groups; critical and non-critical groups. Patients who admitted to the routine ward of hospital and then discharged (n = 909) were considered as non-critical patients. While, the critical group included those who died (n = 104) or were admitted to the intensive care unit (n = 65). This retrospective study was approved by the Ethics Committee of Baqiyatallah University of Medical Sciences, Tehran, Iran, with code: IR.BMSU.REC.1399.024 and the patients were enrolled after giving written informed consents.

CT Protocol and evaluation of chest CT

The images of non-contrast chest CT scan of supine posture and full inspiration in patients. All CT scan examinations were performed with a 16-row detector CT scanner (general electric GE, optima, USA). The detailed parameters for CT acquisition based on COVID-19 low-dose thoracic CT scan protocol were as follows: tube voltage, 100 kVp, 120 mA, slice thickness of 2.5 mm, reconstruction interval of 1.25 mm, pitch 1.75,speed 35 mm/rot, detector configuration 16*1.25, computed tomography dose index 3.5 mGy. The findings of CT scan were evaluated by two radiologists blinded and agreed with the results of images. The inter-rater coefficient agreement between the two radiologists were r = 0.98; P-Value < 0.0001. According to Fleischner Society Nomenclature recommendations (Schoen et al., 2019, Hansell et al.,

2008), the images of initial chest CT scan were assessed for some features of patients, including GGO)Fig. 1), pericardial effusion, crazy-paving pattern (Fig. 2), consolidation (Fig. 3), pleural effusion, reversed halo sign, linear opacities (Fig. 4), intralesional traction bronchiectasis and lymph node enlargement (Schoen et al., 2019). Afterwards, the score of thin-section CT involvement was allotted based on abnormal areas involved to count the extension of lesions (Chang et al., 2005). A score, ranging from 0 to 5, was given to each lobe according to involving, 0 (no involvement); 1 (< 5% involvement); 2 (25% involvement); 3 (26%-49% involvement); 4 (50%-75% involvement) and 5 (> 75% involvement). A score, from 0 to 5, was assigned to each lobe and a total possible score, from 0 to 25.

Statistical analysis:

The results were described as Mean ± SD in continuous variables. Also, frequency and percentage of categorical variables were reported. The Chi-square test was used to evaluate the association between categorical variables. Moreover, the Mann Withney U test and independent T-test was performed to compare means between number of involved lobe and age in two groups. Also, Classification and Regression Tree (CART) method was used to build a risk assessment model predict the critical and non-critical condition of patients using the age, gender, lesion types, specific signs, presence of diffuse opacity, underlying disease, number of involved lobe and total opacity score. The model, known as a machine learning method, includes decision rules that divided variables according to optimal cut-off of values to predict an outcome (Wang et al., 2020). By DT method, the effects of various factors on easy decisions can be obtained to change to complicated algorithms and then risk assessments can be acquired based on the best variables in splitting of decision tree (Batterham et al., 2009). The graphical-based model illustrates a tree structure to explain easier than other techniques in clinical data of public health (Fernandez et al., 2016). In this study, a model was developed to predict the critical and non-critical status of patients by CART method. Afterwards, the k-fold cross-validation method was used to validate the model. The value of K was considered equal to 10. This approach divides the sample into 10 of subsamples (folds = 10). Tree models are then generated, excluding the data from each subsample in turn. For each tree, misclassification risk is estimated by applying the tree to the subsample excluded in generating it. Cross validation produced a single, final tree model which is presented. This model will be used to predicting the critical or non-critical situation of new cases. The cross validated risk estimate for the final tree is calculated as the average of the risks for all of the trees. In decision tree, each fork is a split in a predictor variable and each end node contains a prediction for the outcome variable. Additionally, the Receiver operating characteristic (ROC) analysis was performed to assess the ability of DT model for prediction the critical and non-critical condition. Level of significance for statistical tests was 0.05. The R-4.0.0 software was used for statistical analysis.

Results:

The study population consisted of 1,078 confirmed patients with COVID-19 who underwent CT scans including 169 critical subjects and 909 non-critical subjects. The baseline characteristics and chest CT

features in the patients with COVID-19 according to critical and non-critical status are given in Table 1. The age of participants in critical group was significantly higher than those in the non-critical group (61.24 ± 13.48 vs. 51.47 ± 14.02, $P < 0.001$). The frequency of the involved lobe number in non-critical group is more than critical group, except for the number of lymph nodes less than 1, which was significant between two groups ($P < 0.001$). The result showed that there was a significant relationship between gender, lesions distribution, lesions type, specific signs of high-resolution computed tomography (HRCT), presence of diffuse opacity and underlying disease ($P < 0.001$).

Table 1
Baseline characteristics and chest CT features in patients with COVID-19 based on critical and non-critical status

Parameter	Critical patients (n = 169)	Non-critical patients (n = 909)	Total patients (n = 1078)	*P*-value
Age (years), mean ± SD	61.24 ± 13.48	51.47 ± 14.02	53 ± 14.37	< 0.001[a]
Total opacity score, mean ± SD	13.71 ± 6.26	4.86 ± 3.52	6.24 ± 5.19	< 0.001[a]
Male gender, n (%)	123 (72.8)	614 (67.5)	737 (68.4)	0.179[b]
Lesions distribution, n (%)				< 0.001[b]
Bilateral + Multifocal	165 (97.6)	766 (84.3)	931 (86.4)	
Others	4 (2.4)	143 (15.7)	147 (13.6)	
Lesions type, n (%)				< 0.001[b]
GGO*	13 (7.7)	401 (44.1)	414 (38.4)	
GGO + crazy paving	19 (11.2)	114 (12.5)	133 (12.3)	
Consolidation	12 (7.1)	30 (3.3)	42 (3.9)	
GGO + Consolidation	125 (74)	364 (40)	489 (45.4)	
Specific signs of HRCT#, n(%)				< 0.001[b]
None	78 (46.2)	617 (67.9)	695 (64.5)	
Liner opacity	24 (14.2)	150 (16.5)	174 (16.1)	
Reversed Halo sign	6 (3.6)	43 (4.7)	49 (4.5)	
Pleural effusion	34 (20.1)	21 (2.3)	55 (5.1)	
Interalesional traction bronchiectasis	17 (10.1)	44 (4.8)	61 (5.7)	
Lymphadenopathy	10 (5.9)	34 (3.7)	44 (4.1)	
Presence diffuse opacity, n (%)				

*GGO: ground-glass opacities, # HRCT: high-resolution computed tomography, a: independent-T test, b: Chi-square test, c: Mann Withney U test

Parameter	Critical patients (n = 169)	Non-critical patients (n = 909)	Total patients (n = 1078)	*P*-value
Yes	118 (69.8)	63 (6.9)	181 (16.8)	< 0.001[b]
No	51 (30.2)	846 (93.1)	897 (83.2)	
Number of involved lobe, n (%)				< 0.001[c]
0	51 (30.2)	846 (93.1)	897 (83.2)	
1	1 (0.6)	5 (0.6)	6 (0.6)	
2	33 (19.5)	10 (1.8)	49 (4.5)	
3	35 (20.7)	15 (1.7)	50 (4.6)	
4	30 (17.8)	13 (1.4)	43 (4)	
5	19 (11.2)	14 (1.5)	33 (3.1)	
Underlying disease, n (%)				< 0.042[b]
None	159 (94.1)	882 (97)	1041 (96.6)	
Pulmonary	1 (0.6)	6 (0.7)	7 (0.6)	
Cardiac	8 (4.7)	20 (2.2)	28 (2.6)	
Kidney	1 (0.6)	1 (0.1)	2 (0.2)	

*GGO: ground-glass opacities, # HRCT: high-resolution computed tomography, a: independent-T test, b: Chi-square test, c: Mann Withney U test

The decision tree derived from CART analysis is demonstrated in Fig. 5. This decision tree has a depth of 3 levels from the root node and 3 intermediate nodes, including 6 terminal nodes. Each node represents the probability of being critical/non-critical for the corresponding branches. According to Fig. 5, in order to predict the new patients' status act in such way; first, compare total opacity score with 7.5, if the value was more than 7.5, the patient's lesion type will be checked in the next step. Otherwise, the person's age is compared to 62.5. Then, comparisons with the presented variables will continue in at each nodesplit to reach at a branch, and it will be anticipated the critical or non-critical condition of the patients. The number and percentage of cases are presented at the end of each branch. The mentioned model has a striking prediction of the samples critical condition. The results revealed that 98% of people with a non-critical status (specificity), 72.8% of people with a critical condition are correctly predicted (sensitivity). Also the accuracy index, the percentage of true prediction of the patient's condition correctly, is 93.3

(accuracy). The risk estimate of the presented tree model revealed that the proportion of cases that is incorrectly classified, was 0.068 (with se 0.008), which is acceptable.

Based on Fig. 6, the ROC analysis of DT showed an acceptable power in predicting of status in patients with COVID-19, the area under the ROC curve (AUC) of opacity score in CT was 0.93 (95% CI: 0.909, 0.96, $P < 0.001$).

Discussion:

Coronavirus, the cause of severe acute respiratory syndrome, has rapidly affected a large number of people in all the world. In regard to a number of deaths and serious consequences of disease, it is so remarkable to early diagnosis of patients and timely treatment (Li et al., 2020b). One of the most important signs in these patients is to assess the chest CT scan that indicated imaging signs related to disease advancement, including increase in GGO, interstitial septal thickening and consolidative opacities (Salehi et al., 2020).

In this retrospective study, the chest CT features of 1078 patients with COVID-19 in critical and non-critical cases were reviewed. The liner opacities, pure GGO, mixed GGO with consolidation, and mixed GGO with crazy-paving pattern have been the most frequent types of lesions with involving bilateral and multifocal distribution. The DT model was applied to predict the critical or non-critical situation of new cases. The total opacity score, number of lung lobes involvement and presence diffuse opacity have been regarded noticeable variables by data mining. In the study, the total opacity score has been considered as an important variable. If the variable is lower than 7.5, the next essential variable will be age. As the total opacity score is more than 7.5, lesion type improvement is 0.011 and also lesion type is GGO as well as consolidation, the occurrence of the critical condition will be equal to 82.6. It is worth mentioning, when the total opacity score is less than 7.5 and age of patient is less than 62.5, it is predicted that the percentage of non-critical status of patient will be 98.4.

The age difference between the two groups was statistically significant and the mean age in non- critical patients was lower than the critical group ($P < 0.001$). The results of our study are inconsistent with a study of the two groups, and the time from symptom onset to diagnosis and treatment was less than 3 days and more than 3 days ($P = 0.76$). However, gender was considered as a non-significant variable in both studies ($P > 0.05$), the conflict of the results can be that the sample size of that study was too small (n = 25) (Kobayashi et al., 2013). In a study by Zhou et al. patients were divided into two groups, patients with COVID-19 in the early stage (n = 34) and in progressive stage (n = 28) and the reults showed that there was no significant difference in age and gender (Zhou et al., 2020). Moreover, a study by Shen et al. revealed that the age and gender was not significant difference between two groups of confirmed COVID-19 as severe and non-severe patients (Shen et al., 2020). In a study by Liu et al. cccording to the diagnosis and treatment protocol, patients were divided into two groups: recovery or stabilization (n = 67) and progress (n = 11), and the results of the study were consistent with our study. It means that age was considered significant, but gender was not significant (Liu et al., 2020b).

In both groups of our study, the common types of lesions were mixed GGO with consolidation, mixed GGO with crazy-paving pattern, liner opacities and pure GG. The frequency of pure consolidation and mixed GGO with consolidation lesions showed a significant difference between the groups, these types were more common in critical patients than in non-critical patients, which it means that the virus diffuses into the respiratory epithelium can cause necrotizing bronchitis and diffuse alveolar damage. Also, in critical patients reveled more intralesional traction bronchiectasis and pleural effusion lesions than in the non-critical patients. These extrapulmonary lesions indicate the occurrence of severe inflammation in critical group. The results of our study were consistent with other chest CT studies, similarly we observed the frequent specific signs in critical patients than in the non-critical patients (53.8% vs. 32.1%, $P < 0.001$) (Franquet, 2011, Koo et al., 2018). Although, the reversed halo sign and liner opacities were more frequent in non-critical patients, no significant difference was observed between two groups ($P > 0.05$).

According to the DT model, the total opacity score from the critical group was the fundamental variable for distinguishing the critical group from the non-critical group and its accuracy, sensitivity and specificity was 93.3%, 72.8% and 97.1%, respectively. Our findings were consistent with previous studies that reported the sensitivity and specificity of CT images for the diagnosis of lung lesions from 80–90% as well as 82.8–96% (Li et al., 2020a, Li.L et al., 2020, Liu et al., 2020a).

It is worth to mention the sample size of the study was very large. The first limitation of the study was that the time of chest CT examination and the onest symptom were not simultaneous and therefore it was difficult to summarize the features of CT scan that could be shown during the course of the disease.

Conclusions:

In conclusion the results showed that the chest CT examination was so helpful in identifying pulmonary parenchymal abnormalities in the suspected patients with COVID-19. Total opacity score was the main feature of CT in predicting the percentage of each individual with their own characteristics will suffer from a critical or non-critical situation. The main results of the study showed that 98% of patients with non-critical condition and 72.8% of patients with critical situation were correctly diagnosed.

Abbreviations

ARDS: acute respiratory distress syndrome; **CART:** Classification and Regression Tree; **COVID-19:** coronavirus disease 2019; **CT:** computed tomography; **DT:** decision tree; **GGO:** ground-glass opacities; **HRCT:** high-resolution computed tomography; **ROC:** receiver operating characteristic

Declarations

Acknowledgments

This project was completely supported by Baqiyatallah University of Medical Sciences, Tehran, Iran. Thanks to financial support, guidance and advice from the "Clinical Research Development Unit of

Baqiyatallah Hospital".

Author's contributions

A.V, A.T, M.A.P and R.J performed conception and study design. A.V, R.J, F.R.B, S.R and N.J.J did Data acquisition. S.A, N.B, A.V, S.S, M.AP, R.J, F.R.B and N.J.J contributed in writing the original draft, editing and final approval

Funding

The study funded by Baqiyatallah University of Medical Sciences

Availability of data and materials

data would be available by contacting the corresponding author, after removing the ID, age and gender information to protect the patient's privacy

Ethics approval and consent to participate

This retrospective study was approved by the Ethics Committee of Baqiyatallah University of Medical Sciences, Tehran, Iran, with code: IR.BMSU.REC.1399.024.

Consent for publication

All authors have consented to publication.

Competing interests

None.

References

1. World Health Organization. Clinical management of severe acute respiratory infection when novel coronavirus (nCoV) infection is suspected: interim guidance. Published January 28, 2020. Accessed January 31, 2020. https://www.who.int/publications-detail/clinical-managementof-severe-acute-respiratory-infection-when-novelcoronavirus-(ncov)-infection-is-suspected.
2. 2020. *coronavirus.Report coronavirus cases* [Online]. Available: https://www.worldometers.info/coronavirus [Accessed].
3. BATTERHAM, P. J., CHRISTENSEN, H. & MACKINNON, A. J. 2009. Modifiable risk factors predicting major depressive disorder at four year follow-up: a decision tree approach. *BMC Psychiatry,* 9**,** 75.
4. BHAT, R., HAMID, A., KUNIN, J. R., SABOO, S. S., BATRA, K., BARUAH, D. & BHAT, A. P. 2020. Chest Imaging in Patients Hospitalized With COVID-19 Infection - A Case Series. *Curr Probl Diagn Radiol*.

5. BOETTLER, T., NEWSOME, P. N., MONDELLI, M. U., MATICIC, M., CORDERO, E., CORNBERG, M. & BERG, T. 2020. Care of patients with liver disease during the COVID-19 pandemic: EASL-ESCMID position paper. *JHEP Rep,* 2**,** 100113.
6. CHANG, Y. C., YU, C. J., CHANG, S. C., GALVIN, J. R., LIU, H. M., HSIAO, C. H., KUO, P. H., CHEN, K. Y., FRANKS, T. J., HUANG, K. M. & YANG, P. C. 2005. Pulmonary sequelae in convalescent patients after severe acute respiratory syndrome: evaluation with thin-section CT. *Radiology,* 236**,** 1067-75.
7. FERNANDEZ, L., MEDIANO, P., GARCIA, R., RODRIGUEZ, J. M. & MARIN, M. 2016. Risk Factors Predicting Infectious Lactational Mastitis: Decision Tree Approach versus Logistic Regression Analysis. *Matern Child Health J,* 20**,** 1895-903.
8. FRANQUET, T. 2011. Imaging of pulmonary viral pneumonia. *Radiology,* 260**,** 18-39.
9. HANSELL, D. M., BANKIER, A. A., MACMAHON, H., MCLOUD, T. C., MULLER, N. L. & REMY, J. 2008. Fleischner Society: glossary of terms for thoracic imaging. *Radiology,* 246**,** 697-722.
10. KANNE, J. P. 2020. Chest CT Findings in 2019 Novel Coronavirus (2019-nCoV) Infections from Wuhan, China: Key Points for the Radiologist. *Radiology,* 295**,** 16-17.
11. KIM, H. 2020. Outbreak of novel coronavirus (COVID-19): What is the role of radiologists? *Eur Radiol*.
12. KOBAYASHI, D., TAKAHASHI, O., ARIOKA, H., KOGA, S. & FUKUI, T. 2013. A prediction rule for the development of delirium among patients in medical wards: Chi-Square Automatic Interaction Detector (CHAID) decision tree analysis model. *Am J Geriatr Psychiatry,* 21**,** 957-62.
13. KOO, H. J., LIM, S., CHOE, J., CHOI, S. H., SUNG, H. & DO, K. H. 2018. Radiographic and CT Features of Viral Pneumonia. *Radiographics,* 38**,** 719-739.
14. LI, K., WU, J., WU, F., GUO, D., CHEN, L., FANG, Z. & LI, C. 2020a. The Clinical and Chest CT Features Associated With Severe and Critical COVID-19 Pneumonia. *Invest Radiol,* 55**,** 327-331.
15. LI, M. 2020. Chest CT features and their role in COVID-19. *Radiol Infect Dis*.
16. LI, Y., LIU, X., GUO, L., LI, J., ZHONG, D., ZHANG, Y., CLARKE, M. & JIN, R. 2020b. Traditional Chinese herbal medicine for treating novel coronavirus (COVID-19) pneumonia: protocol for a systematic review and meta-analysis. *Syst Rev,* 9**,** 75.
17. LI.L, QIN .L, XU Z, YIN Y, WANG X, KONG B, BAI J, LU Y, FANG Z, SONG Q, CAO K, LIU D, WANG G, XU Q, FANG X, ZHANG S, XIA J & J., X. 2020. Artificial Intelligence Distinguishes COVID-19 from Community Acquired Pneumonia on Chest CT. *Radiology***,** 200905.
18. LIU, K. C., XU, P., LV, W. F., QIU, X. H., YAO, J. L., GU, J. F. & WEI, W. 2020a. CT manifestations of coronavirus disease-2019: A retrospective analysis of 73 cases by disease severity. *Eur J Radiol,* 126**,** 108941.
19. LIU, W., TAO, Z. W., WANG, L., YUAN, M. L., LIU, K., ZHOU, L., WEI, S., DENG, Y., LIU, J., LIU, H. G., YANG, M. & HU, Y. 2020b. Analysis of factors associated with disease outcomes in hospitalized patients with 2019 novel coronavirus disease. *Chin Med J (Engl),* 133**,** 1032-1038.
20. MATTHAY, M. A., ZEMANS, R. L., ZIMMERMAN, G. A., ARABI, Y. M., BEITLER, J. R., MERCAT, A., HERRIDGE, M., RANDOLPH, A. G. & CALFEE, C. S. 2019. Acute respiratory distress syndrome. *Nat Rev*

Dis Primers, 5**,** 18.

21. MOFTAKHAR, L. & SEIF, M. 2020. The Exponentially Increasing Rate of Patients Infected with COVID-19 in Iran. *Arch Iran Med,* 23**,** 235-238.
22. MUNIZ-RODRIGUEZ, K., FUNG, I. C.-H., FERDOSI, S. R., OFORI, S. K., LEE, Y., TARIQ, A. & CHOWELL, G. 2020. Transmission potential of COVID-19 in Iran. *medRxiv*.
23. MUSA, S. 2020. Hepatic and gastrointestinal involvement in coronavirus disease 2019 (COVID-19): What do we know till now? *Arab J Gastroenterol,* 21**,** 3-8.
24. RODRIGUEZ-MORALES, A. J., CARDONA-OSPINA, J. A., GUTIERREZ-OCAMPO, E., VILLAMIZAR-PENA, R., HOLGUIN-RIVERA, Y., ESCALERA-ANTEZANA, J. P., ALVARADO-ARNEZ, L. E., BONILLA-ALDANA, D. K., FRANCO-PAREDES, C., HENAO-MARTINEZ, A. F., PANIZ-MONDOLFI, A., LAGOS-GRISALES, G. J., RAMIREZ-VALLEJO, E., SUAREZ, J. A., ZAMBRANO, L. I., VILLAMIL-GOMEZ, W. E., BALBIN-RAMON, G. J., RABAAN, A. A., HARAPAN, H., DHAMA, K., NISHIURA, H., KATAOKA, H., AHMAD, T. & SAH, R. 2020. Clinical, laboratory and imaging features of COVID-19: A systematic review and meta-analysis. *Travel Med Infect Dis,* 34**,** 101623.
25. SALEHI, S., ABEDI, A., BALAKRISHNAN, S. & GHOLAMREZANEZHAD, A. 2020. Coronavirus Disease 2019 (COVID-19): A Systematic Review of Imaging Findings in 919 Patients. *AJR Am J Roentgenol***,** 1-7.
26. SCHOEN, K., HORVAT, N., GUERREIRO, N. F. C., DE CASTRO, I. & DE GIASSI, K. S. 2019. Spectrum of clinical and radiographic findings in patients with diagnosis of H1N1 and correlation with clinical severity. *BMC Infect Dis,* 19**,** 964.
27. SHEN, C., YU, N., CAI, S., ZHOU, J., SHENG, J., LIU, K., ZHOU, H., GUO, Y. & NIU, G. 2020. Quantitative computed tomography analysis for stratifying the severity of Coronavirus Disease 2019. *J Pharm Anal*.
28. SONG, Y. Y. & LU, Y. 2015. Decision tree methods: applications for classification and prediction. *Shanghai Arch Psychiatry,* 27**,** 130-5.
29. WANG, Y., SHAN, C., ZHANG, Y., DING, L., WEN, J. & TIAN, Y. 2020. Early Recognition of the Preference for Exclusive Breastfeeding in Current China: A Prediction Model based on Decision Trees. *Sci Rep,* 10**,** 6720.
30. ZHOU, Z., GUO, D., LI, C., FANG, Z., CHEN, L., YANG, R., LI, X. & ZENG, W. 2020. Coronavirus disease 2019: initial chest CT findings. *Eur Radiol*.
31. ZIMMERMAN, R. K., BALASUBRAMANI, G. K., NOWALK, M. P., ENG, H., URBANSKI, L., JACKSON, M. L., JACKSON, L. A., MCLEAN, H. Q., BELONGIA, E. A., MONTO, A. S., MALOSH, R. E., GAGLANI, M., CLIPPER, L., FLANNERY, B. & WISNIEWSKI, S. R. 2016. Classification and Regression Tree (CART) analysis to predict influenza in primary care patients. *BMC Infect Dis,* 16**,** 503.

Figures

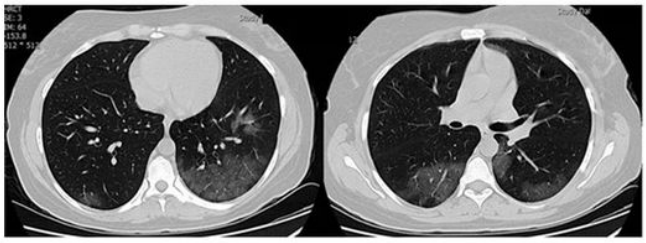

Figure 1

two axial chest CT scan without contrast show bilateral and multifocal patchy sub pleural ground glass opacities (GGO) in a patient with covid-19 pneumonitis

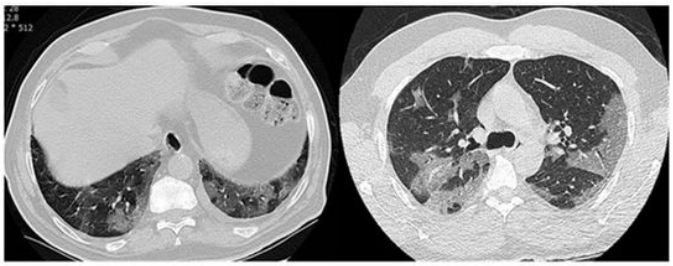

Figure 2

two axial chest CT scan without contrast show multifocal sub pleural patchy ground glass opacities (GGO) with interlobular septal thickening (crazy- paving) at lower lobes of both lung in a patient with covid-19 pneumonitis

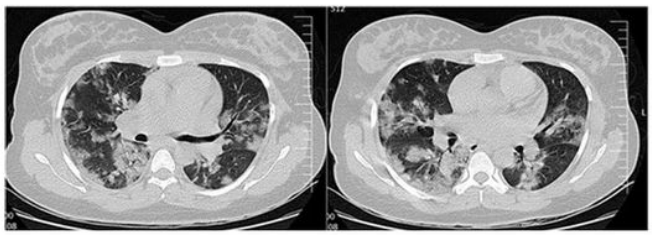

Figure 3

two axial chest CT scan without contrast show bilateral and multifocal patchy consolidation in a patient with covid-19 pneumonitis

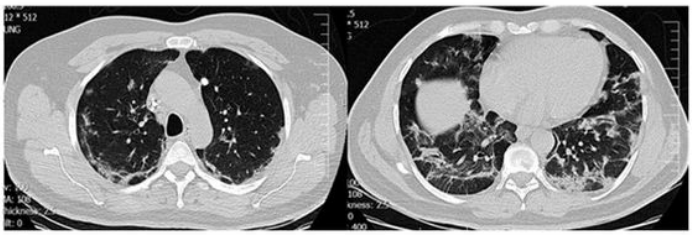

Figure 4

two axial chest CT scan without contrast show bilateral and multifocal linear opacities with architectural distortion in a patient with covid-19 pneumonitis

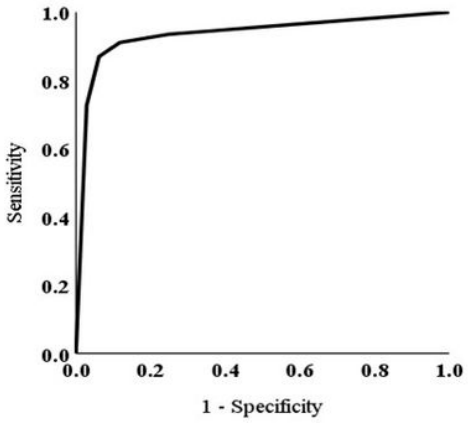

Figure 5

Decision tree predicting the risk for critical or non-critical situation of patients with COVID-19

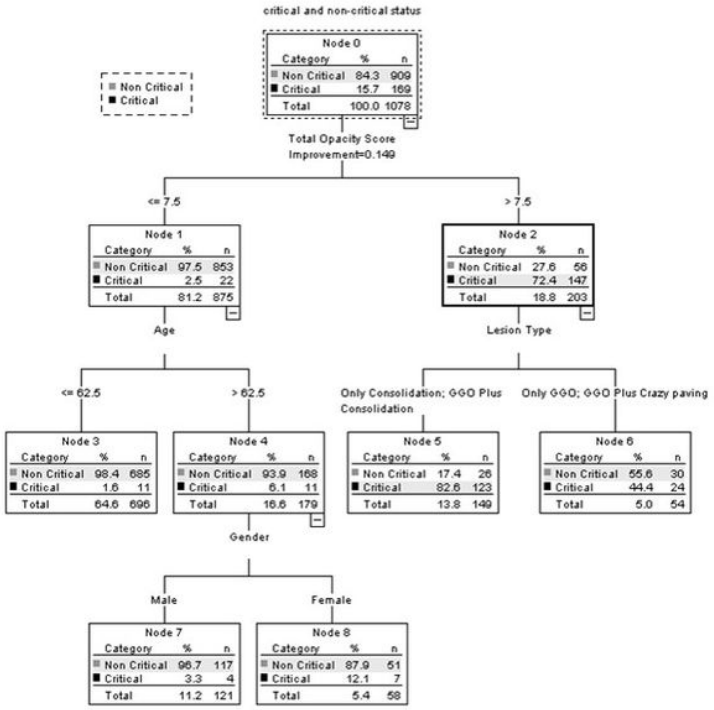

Figure 6

ROC curve for DT, AUC: 93%